UAV remote sensing atmospheric degradation image restoration based on multiple scattering APSF estimation*

QIU Xiang (仇翔)[1,2]**, **DAI Ming** (戴明)[1], and **YIN Chuan-li** (尹传历)[1,2]

1. Changchun Institute of Optics, Fine Mechanics and Physics, Chinese Academy of Sciences, Changchun 130033, China

2. University of Chinese Academy of Sciences, Beijing 100049, China

(Received 15 March 2017; Revised 23 May 2017)

Unmanned aerial vehicle (UAV) remote imaging is affected by the bad weather, and the obtained images have the disadvantages of low contrast, complex texture and blurring. In this paper, we propose a blind deconvolution model based on multiple scattering atmosphere point spread function (APSF) estimation to recovery the remote sensing image. According to Narasimhan analytical theory, a new multiple scattering restoration model is established based on the improved dichromatic model. Then using the L0 norm sparse priors of gradient and dark channel to estimate APSF blur kernel, the fast Fourier transform is used to recover the original clear image by Wiener filtering. By comparing with other state-of-the-art methods, the proposed method can correctly estimate blur kernel, effectively remove the atmospheric degradation phenomena, preserve image detail information and increase the quality evaluation indexes.

Document code: A **Article ID:** 1673-1905(2017)05-0386-6

DOI https://doi.org/10.1007/s11801-017-7074-x

Unmanned aerial vehicle (UAV) remote imaging is influenced by bad weather (fog or haze), illumination variation and motion blur, so the image quality decreases greatly, which seriously impacts its application in environmental monitoring and battlefield reconnaissance field. Currently, most atmospheric remote sensing image restoration algorithms only consider single scattering effect of atmospheric light. The method proposed by He et al[1] using the dark channel principle combined with atmospheric optical physics model can remove the haze to a certain extent, but the color change is not obvious. Wang et al[2] adds minimum and guide filtering based on Ref.[1], which effectively deals with the shadow part of small area in the image, but the algorithm is time consuming. Therefore, Liu et al[3] proposes a fast color conversion method of interval estimation to improve the processing speed and robustness of the algorithm. Due to the long distance between the UAV aerial camera CCD and the captured ground target, the multiple scattering of atmospheric particles cannot be easily ignored, the traditional algorithm[4] based on the Nayar single scattering model[5] is no longer valid, and the results cannot meet the needs of practical engineering. To this end, Pei et al[6] proposed a multiple scattering model based on Bouguers exponential law, which showed that scattering has an effect on the aggregation of all radiance in the neighborhood. Based on the above analyses, we propose a new deconvolution model based on multiple scattering atmosphere point spread function (APSF) estimation, which can significantly improve the speed, keep the clear detail information and remove the artificial ringing effect.

The spectrum can be affected by the absorption and scattering of gas molecules and aerosol molecules in the atmosphere. According to the Bouguers exponential law, with the increase of the aerosol optical thickness, the radiation energy of the scene is attenuated in exponential form. The atmospheric transmittance in homogeneous media can be expressed as

$$t(x) = \mathrm{e}^{-\beta d(x)}, \tag{1}$$

where β denotes the scattering coefficient of the atmosphere medium, and d is the optical depth.

As shown in Fig.1, the absorption of atmospheric particles causes the attenuation of light energy, and the transmission direction of some light is changed several times due to the multiple scattering effect. Therefore, we should consider not only the attenuation of light in the original direction of propagation, but also the increase in other directions.

Nayar[4] assumes that the light that deviates from the

* This work has been supported by the National Natural Science Foundation of China (No.61405191).

** E-mail: yongwuzhifeng@163.com

original propagation direction does not enter the field of view again, so the scattering effect happens only once. A single scattering restoration is modeled as

$$I(x) = J(x)t(x) + A\left[1 - t(x)\right], \tag{2}$$

where x denotes two dimensional coordinate position of a pixel, $I(x)$ is the observed image, $J(x)$ represents scene radiant energy, and A is the atmospheric light.

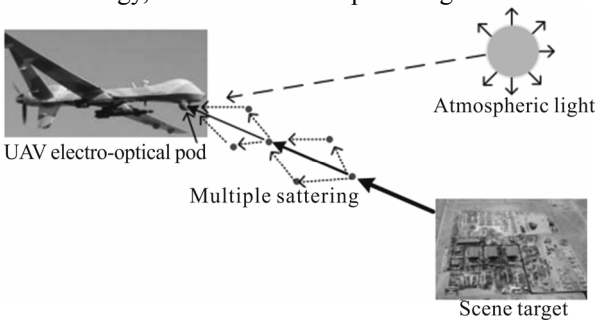

Fig.1 Illustration of multiple scattering in the UAV remote imaging

The above model is ideal for imaging, but in the real environment, such as haze, fog, snow, and other complex weather conditions, the concentration of particles in the atmosphere is too high. The scattered light is most likely to re-enter the field of view. Considering the influence of atmospheric multiple scattering, the amount of radiation received at pixel x is influenced by its neighbour pixels. A point light source is transmitted to the CCD image surface and becomes a diffuse spot, forming blur. As shown in Fig.2, we can use the APSF to describe the redistribution of the point light source on the CCD image plane, and the degradation process can be formed as

$$E_I(x) = E_J(x) \otimes h_A(x), \tag{3}$$

where E_I denotes the actual amount of radiation received by a detector, E_J represents the radiation before the target scene decay, h_A is the degraded atmospheric blur kernel, and $\otimes$ is the convolution operator.

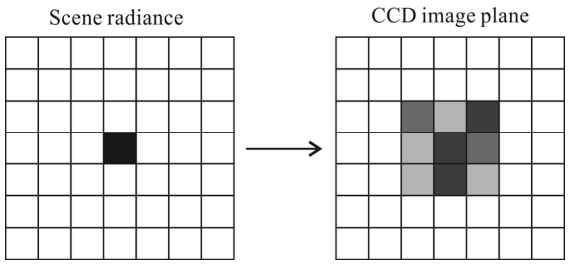

Fig.2 The relation between object and image under the influence of atmosphere

According to Eq.(3), the single scattering restoration model in Eq.(2) can be improved as

$$I(x) = \left[J(x) \otimes h_A\right]t(x) + A\left[1 - t(x)\right], \tag{4}$$

where $\left[J(x) \otimes h_A\right]$ represents the amount of scene radiation affected by multiple scattering effects. The degradation model is more effective for long range imaging and bad weather conditions.

Similar to He et al[1], we use the dark channel prior to solve the atmospheric transmittance. The minimum filter is described as

$$J^{\text{dark}}(x) = \min_{c\in\{r,g,b\}}\{\min_{y\in\Omega(x)}[J^c(y)]\}, \tag{5}$$

where $J^{\text{dark}}(x)$ represents the dark channel of the pixel located at x, J^c denotes color channel, and $\Omega(x)$ is the local area centered at x. The maximum luminance point in the dark color image is selected as the atmospheric background radiation A. If there is no atmospheric interference in the imaging process, Eq.(5) tends to 0, and the transmittance can be obtained by Eq.(4) as

$$t(x) = 1 - \min_{y\in\Omega(x)}\left\{\min_{c\in\{r,g,b\}}\left[\frac{I^c(y)}{A^c}\right]\right\}. \tag{6}$$

Through the above analyses, given A and $t(x)$, Eq.(4) can be converted into the following expression

$$\boldsymbol{B} = (J * t) \otimes h_A. \tag{7}$$

Then in the following description, (J*t) will be recorded as f, and the subscript A is omitted for simplicity, i.e., Eq.(7) becomes

$$\boldsymbol{B} = f \otimes h + n, \tag{8}$$

where $\boldsymbol{B}$ is the blur image, n is an optical device noise, and h is the point spread function (PSF).

Because of the gradient distribution of the blurred image is denser than that of the clear image, and the sparse of the dark channel is relatively small[7], we add the L0 norm sparse priors of gradient and dark channel to propose a novel regularization model to estimate APSF blur kernel as

$$\min_{f,h}\left\|f \otimes h - \boldsymbol{B}\right\|_2^2 + \gamma\left\|h\right\|_2^2 + \mu\left\|\nabla f\right\|_0 + \lambda\left\|D(f)\right\|_0, \tag{9}$$

where the first term is the distance term to ensure the minimum error between the restored image and the observed image, the second term is the penalty term to prevent the optimal solution over-fitting, the third term on image gradients retains large gradients and removes tiny details, and the fourth term is a dark channel prior on the original image. γ, μ and λ are balance parameters.

For Eq.(9), we choose the coordinate descent method to solve the blur kernel h, and convert it into the following two forms as

$$\min_{f}\left\|f \otimes h - \boldsymbol{B}\right\|_2^2 + \mu\left\|\nabla f\right\|_0 + \lambda\left\|D(f)\right\|_0, \tag{10}$$

$$\min_{h}\left\|f \otimes h - \boldsymbol{B}\right\|_2^2 + \gamma\left\|h\right\|_2^2. \tag{11}$$

Because of the existence of the L0 norm and the nonlinear function $D(f)$ in Eq.(10), it is a non-deterministic polynomial (NP) problem. We minimize the L0 norm problem by the half-quadratic splitting method[8], by introducing auxiliary variables $\boldsymbol{u}$ and $\boldsymbol{g}$, then the objective function in Eq.(10) can be rewritten as

$$\min_{f,u,g}\|f\otimes h-\boldsymbol{B}\|_2^2+\alpha\|\nabla f-\boldsymbol{g}\|_2^2+\beta\|D(f)-\boldsymbol{u}\|_2^2+\mu\|\boldsymbol{g}\|_0+\lambda\|\boldsymbol{u}\|_0, \tag{12}$$

where $\boldsymbol{u}$ denotes image dark channel $D(f)$, and $\boldsymbol{g}=(g_w, g_v)$ corresponds to image gradients in the horizontal and vertical directions. α and β are penalty parameters, when they tend to infinity, Eq.(12) is close to Eq.(10). We can solve f, $\boldsymbol{u}$ and $\boldsymbol{g}$ by alternating iteration, respectively. Under the given f, solving auxiliary variables $\boldsymbol{u}$ and $\boldsymbol{g}$ is an element-wise minimization problem[9]. It does not involve nonlinear functions $D(f)$. Thus, the closed solution can be obtained as

$$\boldsymbol{u}=\begin{cases}D(f), & |D(f)|^2\ge\dfrac{\lambda}{\beta},\\ 0, & \text{otherwise}\end{cases} \tag{13}$$

$$\boldsymbol{g}=\begin{cases}\nabla f, & |\nabla f|^2\ge\dfrac{\mu}{\alpha}.\\ 0, & \text{otherwise}\end{cases} \tag{14}$$

Therefore, we only need to deal with the nonlinear minimization problem for solving f:

$$\min_f\|f\otimes h-\boldsymbol{B}\|_2^2+\alpha\|\nabla f-\boldsymbol{g}\|_2^2+\beta\|D(f)-\boldsymbol{u}\|_2^2. \tag{15}$$

In order to convert it into a linear problem, we propose a linear matrix operator $\boldsymbol{M}$ based on look-up tables (LUT) to map the vector image f to the dark channel $D(f)$. Setting $y=\text{argmin}_{z\in N(x)}f(z)$, $\boldsymbol{M}$ satisfies the following conditions:

$$\boldsymbol{M}(x,z)=\begin{cases}1, & z=y\\ 0, & \text{otherwise}\end{cases}. \tag{16}$$

Multiplying the xth row of $\boldsymbol{M}$ with f under the given brightness value of pixel y, $f(y)$ is equivalent to $D(f)(x)$. As shown in Fig.3, the three squares on the intermediate value f are used to calculate the dark elements in the adjacent image patches, where the minimum intensity value in each patch is marked with different colors. Transposed matrix $\boldsymbol{M}$ is an inverse transform.

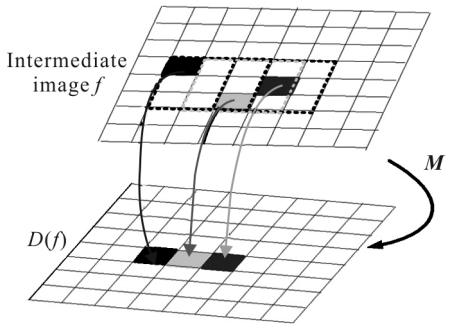

Fig.3 Matrix maps image to dark channel

Thus, $\boldsymbol{M}f=D(f)$ strictly holds. Eq.(15) can be rewritten as

$$\min_f\|\boldsymbol{T}_h f-\boldsymbol{B}\|_2^2+\alpha\|\nabla f-\boldsymbol{g}\|_2^2+\beta\|\boldsymbol{M}f-\boldsymbol{u}\|_2^2, \tag{17}$$

where $\boldsymbol{T}_h$ is the convolution matrix form of h, $\boldsymbol{B}$, $\boldsymbol{g}$ and $\boldsymbol{u}$ represent their vectors, respectively. Through the fast Fourier transform[10], the solution can be obtained as

$$f=F^{-1}\left(\frac{\overline{F(\boldsymbol{T}_h)}F(\boldsymbol{B})+\beta F(\tilde{\boldsymbol{u}})+\alpha(\overline{F(\nabla_w)}F(g_w)+\overline{F(\nabla_v)}F(g_v)}{\overline{F(\boldsymbol{T}_h)}F(h)+\beta+\alpha(\overline{F(\nabla_w)}F(\nabla_w)+\overline{F(\nabla_v)}F(\nabla_v))}\right). \tag{18}$$

Eq.(18) is added to Eq.(11) to alternatively solve the problem, and then the blur kernel h can be obtained. Finally, the Wiener filter is used in the frequency domain to restore the clear image.

In this paper, the experiments are performed using Matlab2014a on a Windows 7 platform with an Intel i7 CPU at 3.3 GHz and 8 GB memory. The parameters of the algorithm are set as γ=2 and λ=μ=0.005, and we adjust λ according to the distance of atmospheric transmission distance. In order to balance accuracy and speed, we set max_*iter*=10. The neighborhood size of calculating dark channel is 35×35. Compared with single scattering restoration models of Wang[2] and Liu[3] and blind deconvolution algorithm of Liao[8], Krishnan[11], Daniel[12], Yu[13] and Pan[14] based on multiple scattering model, recovery effect are analyzed in detail. Finally, the interception of multi frame images from UAV aerial video collected by the small satellite 158HD flight platform are used to further test our method. The restoration image is analyzed by various quality evaluation indexes, and the running time values of these methods are compared.

We perform blur kernel estimation experiments on data sets in Ref.[1]. In Fig.4(a), the city is affected by fog, and the blur kernels estimated by the traditional algorithms have the same shape of the cross star as shown in Fig.4(b)—(f). Fig.4(h) show the severe blurred image influenced by haze and snow. As shown in Fig.4(i)—(m), the error blur kernels estimated by the traditional algorithms are shown as a white stripe with irregular distribution which covers the entire area. But our method can correctly estimate the PSF as shown in Fig.4(g) and (n), and the performance is significantly improved.

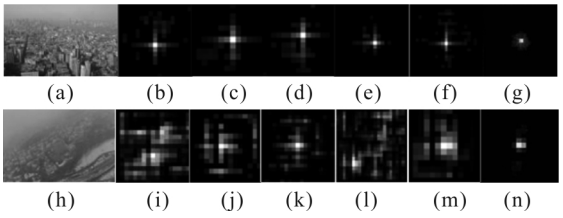

Fig.4 PSF estimation results

Fig.5 shows the results of quantitative analysis. The sum of squared error (*SSD*) values of blur kernel estimated by Krishnan[11], Daniel[12], Pan[14], Liao[8], Yu[13] are too high, and the *SSD* value of our algorithm is obviously decreased, which greatly improves the precision of blur kernel estimation.

Figs.6—8 shows the results of aerial image restoration under three different weather conditions. Fig.6(a) and (g) are the city images affected by fog and haze, Fig.7(a) and

(g) show the images with mountains and clouds, and Fig.8(a) and (g) show the building images under wind and snow conditions, respectively.

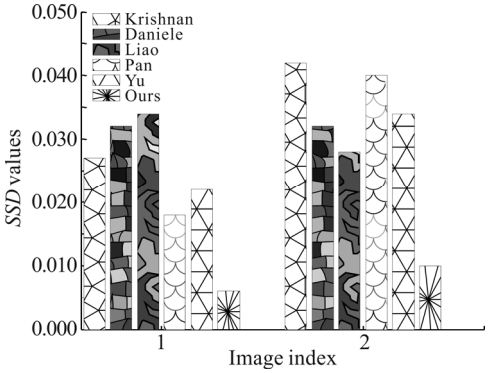

Fig.5 Quantitative analysis comparison

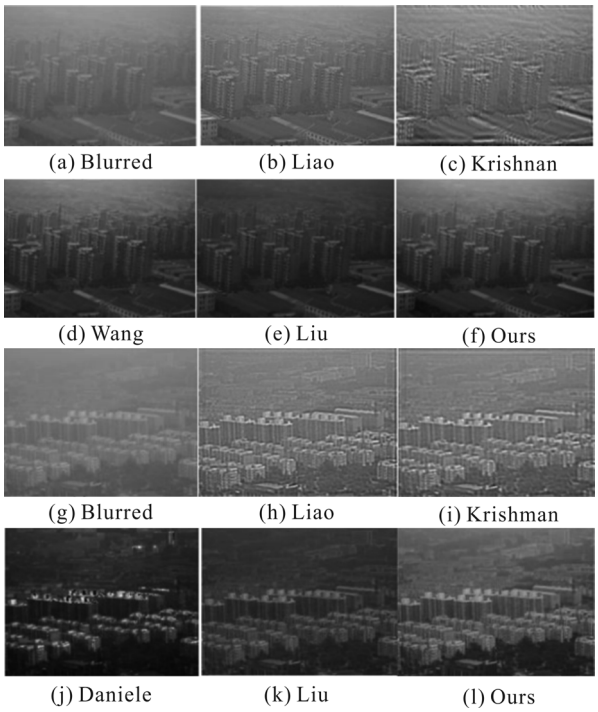

Fig.6 Restoration of aerial city images affected by fog and haze

In images processed by Liu, detail is obvious, but the overall brightness is darker, and smooth effect is poor. The images processed by Daniele have high contrast and gorgeous color, but a serious color cast weakens the details. In images processed by Wang, the color approximates to the true value, the detail information is obvious, but the mountains and woods have the halo effect obviously. The algorithms of Liao and Krishnan have poor ability to resist the Gaussian white noise, and there is a serious artificial ringing effect, some of which are residual blur, the image sharpness decreases, and the texture information lost. The restored images obtained by our algorithm hasve the advantages of moderate brightness and contrast, rich texture details, strong anti-noise ability and good visual effect.

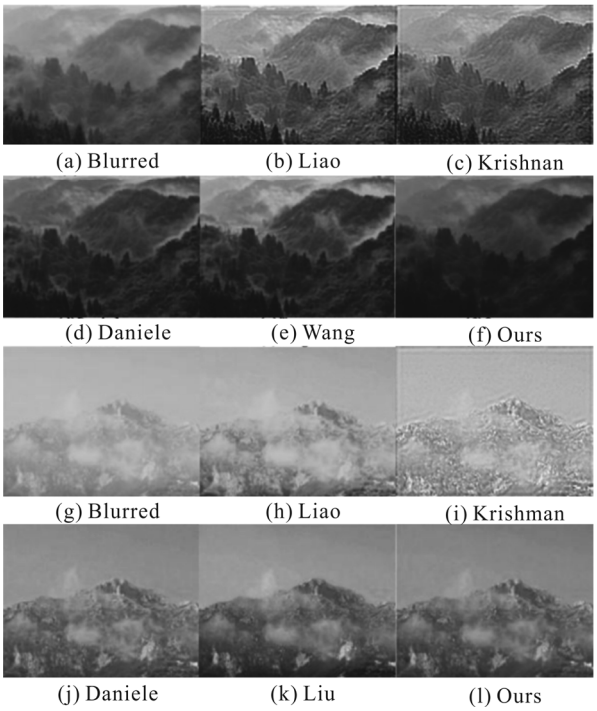

Fig.7 Restoration of images with cloud and mountains

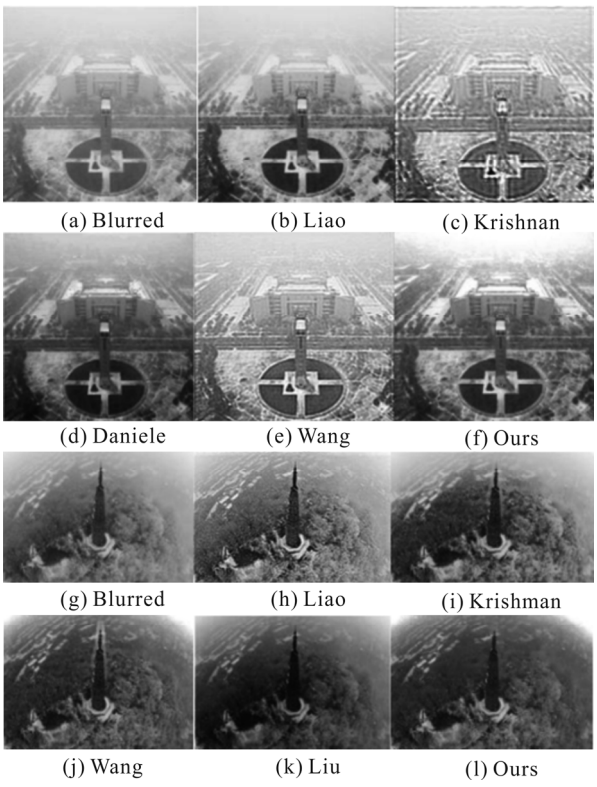

Fig.8 Restoration of aerial images with wind and snow

Fig.9 shows six frame images from UAV aerial video collected by the small satellite 158HD flight platform. As shown in Fig.9(c) and (f), there is a moving target in shooting. The recovery images of Wang have obvious

halo effect around the moving target, such as ships and cars. The recovery images of Krishnan algorithm have serious ringing effect, and the textures of car body and ship are blurred, which greatly affects the recognition of moving targets. Fig.9(b) and (d) show the images taken in rain, the images are gray and white, which interferes with the identification of stationary targets, such as white houses and dams. Daniel algorithm has poor immunity against interference of partial white objects, and appears color cast phenomenon, such as the color of dam, sky and green land. The contrast of image processed by Liu is moderate, and the details are more obvious, but the overall color is darker, and the smoothing effect of the abrupt change of the depth of field is poor, such as dams, sky, the edge of house and the green space, so the whole visual effect is not in a good quality. For the remote images shown in Fig.9(a) and (e), light transmission process is longer, so the effect of atmospheric particle scattering is more obvious. Because the contrast of three regions in the original image is strong, such as waters, green land and soil, the algorithms of Pan and Yu can effectively estimate the blur kernel by using the natural gradient priors, and only a small part of the region is slightly foggy, the overall contrast is moderate, and the recovery effect is good. For the above images, it is observed that our algorithm is better than the current state-of-the-art recovery algorithm, and our algorithm can basically solve the UAV remote sensing image restoration.

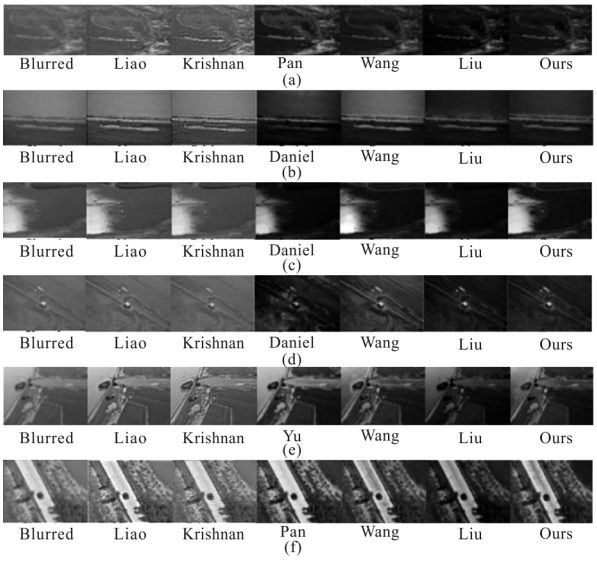

Fig.9 UAV aerial image restoration

This paper adopts five kinds of objective evaluation index[15,16], which are the mean brightness (*GM*), contrast, gray mean gradient (*GMG*), Laplacian sum (*LS*) and information entropy (*H*), to quantitatively evaluate UAV remote sensing atmospheric degradation restoration image of the above six frames. The average evaluation indexes and the running time of the compared algorithms are shown in Tab.1.

Tab.1 Performance evaluation results of algorithms

Methods	*GM*	Contrast	*GMG*	*LS*	*H*	Time (s)
Liao	86.354	6.216	8.647	5.675	4.647	12.78
Krishnan	76.458	5.267	4.971	3.148	3.971	22.45
Daniel	47.164	9.697	10.657	6.634	5.113	15.34
Pan	64.187	12.364	11.323	10.147	6.657	8.62
Yu	68.549	14.679	10.667	7.941	5.984	6.25
Wang	58.647	16.213	12.637	8.617	6.314	3.64
Liu	52.416	13.698	12.425	9.671	7.147	4.68
Ours	70.367	18.677	13.687	12.367	8.679	3.08

It is observed that our algorithm can significantly improve all indexes, and the results are consistent with the subjective evaluation. Due to our method based on L0 norm regularization model and the L1 norm total variation regularization method of Daniel are relatively close on mathematical theory, which all obtain the optimal solution by using the prior condition, so the results are similar. The method of Daniel is a simple mathematical problem which is based on Bayesian principle to filter the trivial solution. While we explore the physical properties of the image in all kinds of weather, the natural priors of image gradient and dark channel are added, so our result is better than Daniele's in actual atmosphere degraded image restoration project. The speed of our algorithm is several times faster than those of regularization methods of Krishnan and Daniel. Compared with the ratio regularization of Liao and Yu, there is a significant improvement, but we also need to calculate the image of dark channel, the main spending time is slightly better than those of single scattering physical model algorithm of Wang and Liu. Our algorithm is accelerated by fast Fourier transform (FFT). The processing time on a 512×512 image is only about 3 s.

We propose a new blind deconvolution model based on multiple scattering APSF estimation for remote sensing image restoration, and it can effectively remove the atmospheric degradation under complex weather conditions. Our multiple scattering restoration model can perfectly describe the physical characteristics of atmospheric transmission by using the L0 norm sparse priors of gradient and dark channel estimate APSF blur kernel to restore the original clear image. The experimental results show that the restored image retains the details, greatly improves the operation speed, and can effectively suppress the ringing effect at the edge of image. The contrast, *GMG*, *LS* and information entropy are significantly improved, which are all superior to those of the state-of-the-art algorithms.

References

[1] K. M. He, J. Sun and X. O. Tang, Single Image Haze Removal Using Dark Channel Prior, IEEE Conference

on Computer Vision and Pattern Recognition, 1956 (2009).

[2] WANG Wei-xing, XIAO Xiang and CHEN Liang-qin, Optics and Precision Engineering **23**, 2100 (2015). (in Chinese)

[3] LIU Hai-bo, YANG Jie and WU YA-ping, Journal of Electronics and Information Technology **33**, 381 (2016). (in Chinese)

[4] LIU Yan, ZHANG Hong-ying and WU Ya-dong, Journal of Graphics **36**, 68 (2015). (in Chinese)

[5] S. Nayar and S. Narasimhan, International Journal of Computer Vision **48**, 233 (2002).

[6] P. Wei, Y. Liu and S. Wang, Dehazing Model Based on Multiple Scattering, International Congress on Image and Signal Processing, 249 (2010)

[7] J. S. Pan, D. Q. Sun, H. Pfister and M. H. Yang, Blind Image Deblurring Using Dark Channel Prior, IEEE Conference on Computer Vision and Pattern Recognition, 1628 (2016).

[8] LIAO Yong-zhong, CAI Zi-Xing and HE Xiang-hua, Optics and Precision Engineering **23**, 2086 (2015). (in Chinese)

[9] L. Xu, H. Zheng and J. Jia, Unnatural L0 Sparse Representation for Natural Image Deblurring, IEEE Conference on Computer Vision and Pattern Recognition, 1107 (2013).

[10] S. Cho, S. Paris, B. K. P. Horn and W. T. Freeman, Blur Kernel Estimation Using the Radon Transform, IEEE Conference on Computer Vision and Pattern Recognition, 241 (2011).

[11] D. Krishnan, T. Tay and R. Fergus, Blind Deconvolution Using a Normalized Sparsity Measure, IEEE Conference on Computer Vision and Pattern Recognition, 233 (2011).

[12] D. Perrone and P. Favaro, IEEE Transactions on Pattern Analysis and Machine Intelligence **10**, 8162 (2015).

[13] YU Yi-Bin, PENG Nian and GAN Jun-Ying, Acta Electronica Sinica **44**, 1168(2016). (in Chinese)

[14] J. S. Pan, Z. Hu, Z. X. Sun and M. H. Yang, IEEE Transactions on Pattern Analysis and Machine Intelligence, **10**, 255 (2016).

[15] Z. Hu, S. Cho, J. Wang and M.-H. Yang, Deblurring Low-Light Images with Light Streaks, IEEE Conference on Computer Vision and Pattern Recognition, 3382 (2014).

[16] N. Wang, J. Ding, L. Chen and R. Chang, Efficient Image Deblurring via Blockwise Non-Blind Deconvolution Algorithm, International Conference on Information Communications and Signal Processing, 1 (2015).